PHYSICAL REVIEW A VOLUME 36, NUMBER 7 OCTOBER 1, 1987

Cross sections for electron capture and loss. II. H impact on H and H_2

M. W. Gealy* and B. Van Zyl
Department of Physics, University of Denver, Denver, Colorado 80208
(Received 27 April 1987)

The electron-capture and electron-loss reactions for H impact on H and H_2 have been examined for projectile energies between 2.0 and about 0.1 keV. Relative cross sections for these reactions were measured directly, and the data for H targets were placed on an absolute scale by normalizing to the available results for H_2 targets. For the electron-capture (ion-pair formation) reaction, some new data are also reported here for H_2 targets. The crossed-beam techniques used to accomplish the measurements are described, and the results are compared with other experimental and theoretical data where possible.

I. INTRODUCTION

Relative values of the electron-capture cross sections (σ_{0-1}) and the electron-loss cross sections (σ_{01}) have been measured for H impact on H and H_2 targets. The H-energy ranges covered were from 2.0 to 0.063 keV for σ_{0-1}, and 2.0 to 0.125 keV for σ_{01}. The data for H-atom targets were placed on an absolute scale by use of the results of Van Zyl *et al.*[1] for H_2 targets as standards, although improved values of σ_{0-1} for H_2 targets were measured here for H energies between 2.0 and 0.35 keV. This work is an extension of that described in the preceding paper[2] (henceforth referred to as paper I) where similar data were reported for H^+ and H^- impact on H and H_2.

We were motivated to make these measurements for a variety of reasons. The H + H interactions leading to H^+ and H^- formation are obviously the simplest examples of such charge-changing reactions that can occur, and should thus be of basic interest as a testing ground for theoretical analyses. This is particularly true for our relatively low range of collision energies, where the molecular aspects of the interactions must be considered. We have also found previously[1,3] that the cross sections for ion-pair formation in such reactions as $H+H_2\rightarrow H^-+H_2^+$ and $H+Ar\rightarrow H^-+Ar^+$ exhibit large structures at low H energies, often dominating over other reaction channels leading to charged-particle formation. No data were available to determine if a similar situation would occur in H + H interactions which, presumably, should be theoretically accessible.

Such data should also find practical applications in understanding various astrophysical phenomena, stellar and hydrogen-rich planetary atmospheres, and thermonuclear-fusion test devices, to name but a few. Finally, as noted in paper I, we plan to extend these results to include data for O-atom targets and, eventually, to study collisional-excitation processes as well.

II. EXPERIMENTAL APPARATUS

The basic apparatus used to make the measurements reported here has been described in Sec. II of paper I. The reader is encouraged to review this material, for only those aspects of the apparatus particular to these specific measurements are discussed below.

The fast H projectiles used for these studies were produced by photodetaching electrons from H^- ions, i.e., by the reaction

$$H^-+h\nu\rightarrow H+e^- . \quad (1)$$

The light source employed was an yttrium-aluminum-garnet laser (1060 nm) with "perfectly reflecting" end mirrors. H^- ions, after being brought to their desired energy and trajectory, passed through the laser cavity itself, thus greatly increasing the available photon flux. The advantages of using this technique to produce a collimated beam of ground-state H atoms have been discussed elsewhere.[4]

The optical axis of the laser intersected the H^--beam axis 1.5 cm beyond the 9° beam bend discussed in Sec. II of paper I. The remaining H^- ions were electrostatically diverted from the H-beam trajectory to the auxiliary ion collector described in paper I, to determine and monitor the H-beam intensity.[4]

The H projectiles then continued towards their intersection with the target beam,[5] as shown in Fig. 1 of paper I. After traversing the target beam, they impinged on the (copper) surface of the secondary-electron-emission detector, which could also be used to monitor their intensity. Fast forward-scattered H^+ and H^- produced in the interaction region were deflected to their respective collectors by the charge-state separators shown in Fig. 2 of paper I. Thus, at least in principle, these measurements could be carried out in the same way as those made using H^+ and H^- projectiles.

Unfortunately, however, the reaction-product signals here were found to be orders of magnitude smaller than those resulting from ion impact on H and H_2 targets. The available H-atom-beam intensity (typically about 5×10^{10} atoms/sec) was only a few percent of the ion-beam intensities used, and the reaction cross sections to be measured were several orders of magnitude smaller than their ion-impact counterparts. Furthermore, at the lower H energies, not all the product ions could even be collected (as will be discussed below). It was thus neces-

sary to measure ion signals which, under extreme conditions, were as small as 2×10^{-16} A.

The measurement of signals down to this level was, by itself, not a problem for the ultrasensitive electrometer used.[6] A problem, however, did arise in isolating these desired signals from those resulting from the virtual "sea" of electrons and ions present in the scattering chamber under normal operating conditions. These background charged particles resulted largely from impact of scattered H atoms on various surfaces along the beam trajectory. (Remember that the H-atom-beam intensity was up to 8 orders of magnitude larger than these desired signals.) Also present, moreover, was a flow of ions (about 10^{-8} A) from the furnace chamber itself, whenever the furnace was operated at elevated temperatures.[7]

Numerous procedures were used to minimize these background signals. For example, the potentials applied to the charge-state separators (see Fig. 2 of paper I) could be unbalanced (i.e., not operated symmetrically at $\pm V$), to exert some control over the trajectories of these background charged particles in the region near the collector front apertures.[8] Small potentials could also be applied to these apertures themselves. The (negative) potentials on the secondary-electron suppressors inside the collector housings could be varied, at least within some limits.[9] Thus, while it was sometimes quite time consuming, we were able to find suitable operating conditions under which these background signals could be reduced to tolerable levels, so that their effects could be subtracted out to obtain the reaction signals of interest, as will be discussed below.

III. MEASUREMENT TECHNIQUES AND DIAGNOSTICS

For the measurements described in paper I with ion projectiles, it was found convenient to be able to "switch off" the ions just prior to their arrival at the interaction region, using the ion deflectors shown in Fig. 2 of paper I. Together with use of the bypass mode for introducing gas into the furnace chamber, this allowed separation of the measured H-atom signals into those resulting from ion impact on the target-beam particles, and those from ion impact on the residual-hydrogen and jet particles present in the scattering chamber and interaction region. (Such terms as the residual-hydrogen particles, the jet particles, and the bypass mode of operation are defined in Sec. III of paper I.)

Obviously, it would not be possible to use these deflectors in the same way for this study with H projectiles. However, when on, these deflectors would divert ions produced upstream from aperture A (see Fig. 2 of paper I), preventing their collection. Thus, our plan for making these measurements was to subtract the measured deflectors-on ion signals observed with gas in the bypass mode from those observed in the mode with gas introduced into the furnace tube (under the conditions described in Sec. III of paper I, where the jet and residual-hydrogen densities in the scattering chamber had been matched in these modes). This would allow determination of the ion signals resulting from the reactions of interest.

Unfortunately, our discovery that the jet and residual hydrogen particles present in the scattering chamber were partially dissociated when gas was introduced via the hot-furnace tube [demonstrated by the data in Fig. 5(a) of paper I] prevented use of this plan. This resulted from the fact that the dissociation fraction of these particles could not be matched in these two modes of operation.[10]

We thus decided to examine the possibility of not even trying to separate out the ion signals resulting specifically from H impact on the target-beam particles themselves. Rather, we would measure the total (deflectors on) ion signal[11] resulting from H impact on a "composite" target, consisting of all the target-beam, residual-hydrogen, and jet particles present in the region basically defined by the H-atom path between apertures A and B shown in Fig. 2 of paper I. (It was possible to do this only because we had so carefully determined these particle densities and their dissociation fractions via the diagnostic studies described in Sec. III of paper I.)

While we will not present the algebra,[10] it is possible to show that the desired cross-section ratio σ_a/σ_m, using the same notation as in paper I, obtained from the measured (gas in furnace tube, deflectors on) signal ratio $S_f(T)/S_f(T_0)$, can be written as

$$\frac{\sigma_a}{\sigma_m}=\left[\frac{N_{\rm ca}(T)}{N_{\rm cm}(T_0)}\right]^{-1}\left[\frac{S_f(T)}{S_f(T_0)}-\frac{N_{\rm cm}(T)}{N_{\rm cm}(T_0)}\right], \quad (2)$$

similar in form to Eq. (3) in paper I. Here, the effective composite atomic and molecular target-density ratios can be shown to be

$$\frac{N_{\rm ca}(T)}{N_{\rm cm}(T_0)}=\frac{L_rN_{\rm ra}(T)+L_jN_{\rm ja}(T)+L_tN_{\rm ta}(T)}{L_rN_{\rm rm}(T_0)+L_jN_{\rm jm}(T_0)+L_tN_{\rm tm}(T_0)}, \quad (3)$$

$$\frac{N_{\rm cm}(T)}{N_{\rm cm}(T_0)}=\frac{L_rN_{\rm rm}(T)+L_jN_{\rm jm}(T)+L_tN_{\rm tm}(T)}{L_rN_{\rm rm}(T_0)+L_jN_{\rm jm}(T_0)+L_tN_{\rm tm}(T_0)}. \quad (4)$$

The L's are the appropriate path lengths along the H-beam axis over which detectable ion signals can be produced, and the N's are the relative particle densities along these paths. (Read the subscripts ra and rm as "residual atoms" and "residual molecules," respectively, and similarly for the jet and target-beam particles.)

Using the known values of these H-atom path lengths, and the various relative densities found by the measurements described in Sec. III of paper I, we can evaluate Eqs. (3) and (4) as functions of furnace temperature. For $T=2400$ K, these composite density ratios are both about 0.41, so that this composite target still has an effective dissociation fraction of 0.5. This was regarded as sufficient to provide the needed sensitivity for the σ_a/σ_m measurements.

We were also pleased to find that the use of Eq. (2) to determine these σ_a/σ_m was much less sensitive to the uncertainties we assigned to the various relative target densities than we had anticipated. For example, suppose the dissociation fraction of the particles in the jet was

20% larger than our estimated value (near the upper limit assigned in Sec. III of paper I). We would thus need to increase $N_{ja}(T)$ in Eq. (3), and decrease $N_{jm}(T)$ in Eq. (4), relative to $N_{jm}(T_0)$. However, these changes increase $N_{ca}(T)/N_{cm}(T_0)$ and decrease $N_{cm}(T)/N_{cm}(T_0)$ by only a few percent. Furthermore, because of the way these composite density ratios enter Eq. (2), the effects of these changes tend to cancel each other. This is particularly true for measured signal ratios $S_f(T)/S_f(T_0)$ in the range between 0.53 and 1.22, which included all the data obtained here.

By performing such analyses, we were able to conclude that the uncertainties in σ_a/σ_m resulting from the uncertainties found for these composite density ratios should not exceed $\pm 7.8\%$ for any of the data reported here. As in paper I, we again attempt to evaluate all such uncertainties at a 90% confidence level (CL) or higher.

This uncertainty, however, does not include the uncertainties in the measured $S_f(T)/S_f(T_0)$ themselves. As noted in Sec. II, we were sometimes faced here with the need to measure very small signals, and to subtract out a variety of background effects.[7,8,11] After some experimentation, we devised a procedure that, while tedious, was quite effective for obtaining these desired $S_f(T)/S_f(T_0)$.

This procedure consisted of three basic steps, but involved a large number of separate measurements for each data point.[10] We began by recording "signal" with both the fast H beam and the target beam off.[12] Measurements were next made with only one or the other of the beams on, and then with both on. This sequence was then repeated in reverse order. Step 2 involved making all these same measurements (those with both beams on twice) at elevated furnace temperature (usually near 2400 K). They were then all repeated a third time as step 3 at room temperature, after allowing a few minutes for the furnace to cool. (This procedure usually took about 1.2 h.) The appropriate signal subtractions were then made, and the results of step 2 used to find two values of $S_f(T)$. The results of steps 1 and 3 were also used to obtain two values of $S_f(T_0)$, and to examine the quality and acceptability of the data run.[13]

When the data from many such runs (sometimes more than 10) were combined, it was possible to find $S_f(T)/S_f(T_0)$ to within (90% CL) uncertainties generally ranging between about $\pm 4\%$ and $\pm 16\%$. Unfortunately, however, use of Eq. (2) to determine σ_a/σ_m from such data resulted in magnification of these uncertainties, because of the required subtraction of $N_{cm}(T)/N_{cm}(T_0) \simeq 0.41$ from these measured signal ratios. Fortunately, where these signal ratios were found to be the smallest (near 0.53, for the σ_{01} data at high H energies), they could be measured the most accurately (the signals themselves being quite large and well above the troublesome background effects here). Nevertheless, the uncertainties from this source generally dominated over all others for these σ_a/σ_m measurements.

For the case of H^+ or H^- impact on H_2, we were able to show in Sec. III of paper I that the collisional production of H atoms was accompanied with little angular scattering, even at the lower projectile energies. However, based upon our previous studies of H^+ and H^- formation during H-impact collisions,[1,3] we knew that, below some H energy, some of these reaction products would be angularly scattered beyond the limits of detection here (i.e., beyond about ± 4 degrees from the center of the interaction region). We now discuss the magnitude of this problem, and its impact on these σ_a/σ_m measurements.

Van Zyl *et al.*[1] have measured σ_{01} for $H+H_2$ collisions for H energies between 2.5 and 0.063 keV. These results are compared in Fig. 1 with those reported by Smith *et al.*[14] for H energies down to 0.25 keV, and with the data of Stier and Barnett,[15] McClure,[16] and Hill *et al.*[17] at higher H energies.[18] As can be seen, these data are all in reasonable agreement, leaving little doubt about the magnitude and H-energy dependence of this cross section.

We thus began our studies of the angular scattering occurring in these ion-forming collisions by measuring an "apparent" σ_{01} for H impact on H_2, to compare with these data. If some of the H^+ produced in the interaction region were scattered beyond detectable limits, we would expect that this apparent σ_{01} would lie below these other data by an amount indicative of this problem. The results of this study are also included in Fig. 1, where the apparent σ_{01} data shown have been normalized to the data of Van Zyl *et al.*[1] at 2-keV H energy.[19] As can be seen, for H energies above 0.7 keV, these apparent σ_{01} values agree quite well with the other available data. Below this energy, however, they begin to decrease more rapidly, diverging from the other data at lower H energies E by an amount scaling roughly as E^{-1}, typical of such scattering phenomena.[1,3]

In view of this finding, we decided to make a similar study of the σ_{0-1} data for $H+H_2$ collisions, to see if the product H^- were angularly scattered by a generally

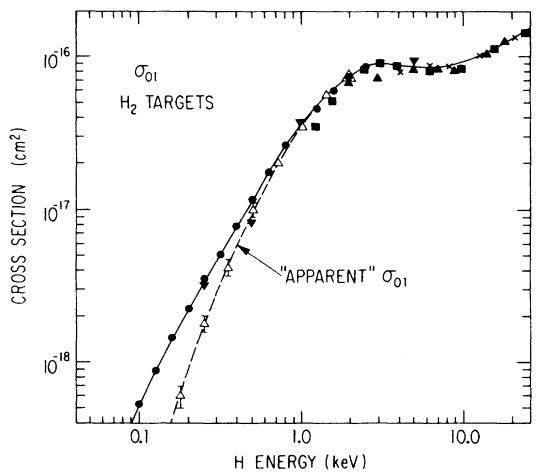

FIG. 1. Electron-loss cross sections for H impact on H_2. The measured data are from ●, Van Zyl *et al.* (Ref. 1); ▼, Smith *et al.* (Ref. 14); ×, Stier and Barnett (Ref. 15); ■, McClure (Ref. 16); and ▲, Hill *et al.* (Ref. 17). The apparent σ_{01} values measured here, ∇, are shown for comparison.

comparable amount. The results of this investigation are shown in Fig. 2, where the data of Van Zyl *et al.*[1] are compared with those of Stier and Barnett,[15] McClure,[20] and Hill *et al.*[17] at the higher H energies.[18] Also shown again are the apparent σ_{0-1} measured here.[21]

Note that, for H energies below about 0.4 keV, our apparent σ_{0-1} values again fall increasingly below the data of Van Zyl *et al.*[1] by amounts, in fact, which are quite close to those shown in Fig. 1 for the σ_{01} data. However, for H energies above 0.4 keV, these apparent σ_{0-1} values actually lie above the data of Van Zyl *et al.*[1] Indeed, even at 2-keV H energy, the apparent $\sigma_{0-1}=6.91\times10^{-18}$ cm^2 found here[21] is 17% above the value of Van Zyl *et al.*,[1] and close to 1.6 times that of McClure.[20] (Consideration of other available data[18] does little to resolve this discrepancy. For example, the value of Williams[22] is less than 40% of that found here.) Our apparent σ_{0-1} value, however, is in excellent agreement with the 6.70×10^{-18} cm^2 reported by Hill *et al.*,[17] which is probably the most accurate result available (the uncertainty cited being only $\pm7.5\%$).

In defense of the σ_{0-1} reported by Van Zyl *et al.*[1] for H energies above about 0.4 keV, which we believe to be incorrect, it must be noted that these data suffered from a multitude of measurement difficulties. These resulted largely from the need to obtain these (small) cross-section values by subtraction of two large (but not very different) signals. In addition, the data had to be adjusted to account for the loss of H^- signal because of angular scattering effects, which could not be directly evaluated by the measurement procedures used. In fact, in contrast to their σ_{01} data, Van Zyl *et al.*[1] did not even attempt to assign uncertainties to these σ_{0-1} measurements, which were presented only in the spirit of indicating the general trend of this cross section with H energy.

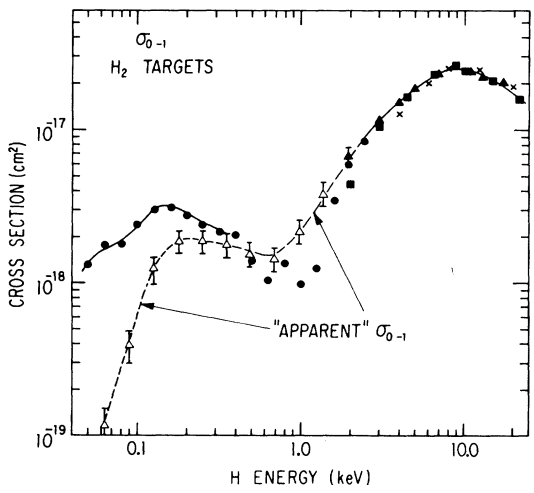

FIG. 2. Electron-capture cross sections for H impact on H_2. The measured data are from ●, Van Zyl *et al.* (Ref. 1); × Stier and Barnett (Ref. 15); ■, McClure (Ref. 20); and ▲, Hill *et al.* (Ref. 17). The apparent σ_{0-1} values measured here, ▽, are shown for comparison.

In contrast, for H energies below 0.4 keV, the σ_{0-1} data of Van Zyl *et al.*[1] should be more accurate. Here the ion-pair-formation reaction under study,

$$H+H_2\rightarrow H^-+H_2^+ , \tag{5}$$

becomes the dominant mechanism for H_2^+ formation during the collisions, having a cross section much larger than that for[23]

$$H+H_2\rightarrow H+H_2^++e^- . \tag{6}$$

Thus, at low H energies, $\sigma_{0-1}\simeq\sigma_t(H_2^+)$, the total cross section for H_2^+ formation, and Van Zyl *et al.*[1] used the more accurately measured $\sigma_t(H_2^+)$ to determine their σ_{0-1} here.

After weighing all these data, we decided we had little choice but to use our measured apparent σ_{0-1} values for H energies above 0.4 keV to determine the actual σ_{0-1} for $H+H_2$ collisions. We thus assumed that, in this H-energy region, the fractions of the total H^- which were scattered beyond detectable limits were similar to those found for H^+ from the data plotted in Fig. 1, and our apparent σ_{0-1} were adjusted accordingly. This did result in σ_{0-1} values which merged smoothly onto the data of Van Zyl *et al.*[1] at the lower H energies where, as noted above, these data should again become valid.

As can be seen in Figs. 1 and 2, at low H energies, substantial fractions of the reaction-product H^+ and H^- produced in $H+H_2$ collisions were being scattered beyond detectable limits. By itself, this presented no obstacle to measuring the σ_a/σ_m of interest here, under the assumption that the fractions of the reaction-product ions collected were the same for H impact on both H and H_2 targets. The experimental verification of this assumption was probably the most difficult part of this measurement program.

As discussed in Sec. II of paper I, the entire collector assembly could be rotated about an axis near the center of the charge-state separators, in part to allow study of such reaction-product angular scattering effects. This proved to be a useful tool to investigate scattering of product H atoms resulting from ion impact on H and H_2 (although as noted in paper I, no evidence of any significant scattering was ever found). During these ion-impact studies, the charge-state-separator difference potential was adjusted as the collectors were rotated, so that the primary beam ions were always directed into their respective collectors.

Unfortunately, this could not be done when using the primary H-atom beam. Therefore, when the collectors were rotated by more than about 4°, the primary H atoms began to impact the front aperture of their collector. Here, they released (relatively) enormous numbers of secondary electrons and ions, causing the signals from these background charged particles[8] to overwhelm those of interest.

However, we could also keep the collector assembly in its normal position and use the difference potential on the charge-state separators to direct product ions leaving

the interaction region at various scattering angles into their appropriate collector. While this circumvented the problem noted above, it did require searching for suitable operating conditions (as discussed in Sec. II) every time these charge-state-separator potentials were changed.

In Fig. 3 we show the result of one study made using a combination of the techniques described above. Here we have plotted the relative values of the measured $S_f(T_0)$ and $S_f(T)$ signals (read the left ordinate label) as functions of the approximate scattering angle of the H^- produced in the interaction region for 0.177-keV H energy. We have called this an "approximate scattering angle" because of the integrating effect of the H^- collector which, as noted above, accepted H^- particles scattered within a 4° half-angle cone. In other words, these data basically represent relative differential cross sections measured with very poor angular resolution.

Note that the decrease of both $S_f(T_0)$ and $S_f(T)$ with increasing scattering angle is very similar. This is further illustrated by the signal ratio $S_f(T)/S_f(T_0)$, also plotted in Fig. 3 (read the right ordinate label). As can be seen, this signal ratio, and thus the σ_a/σ_m as derived from Eq. (2), appears to be independent of the reaction-product H^- scattering angle, at least to within measurement statistics. Although the statistical spread in these signal-ratio data at the two largest scattering angles is quite large, consideration of this total set of results led us to judge that this conclusion was valid to within a ±5% uncertainty.[24]

While it was comforting to be able to confirm this experimentally, we had anticipated that this would be our finding. Over most of the range of H energies covered here, any large-angle scattering must result from fairly close nuclear encounters (particularly for these unit-charge nuclei). Thus, the (nuclear) impact parameter must be small compared to the H_2 internuclear separation, so that such scattering should be similar for H impact on H or H_2 targets.

At the very low H energies, of course, this argument begins to break down. Here, we might expect the H projectile to be scattered by some combination of the two H_2 nuclei (depending on the molecular orientation during the collision), resulting in more scattering from H_2 than from H targets. Remember, however, that the center-of-mass energy for H impact on H_2 is larger than for H impact on H, tending to counter the above effect, so that such scattering should still not be profoundly different. We thus concluded that, to within our assigned uncertainties,[24] the σ_a/σ_m measured here should not be seriously influenced by such reaction-product-scattering effects. (We will also provide some more evidence for this conclusion later.)

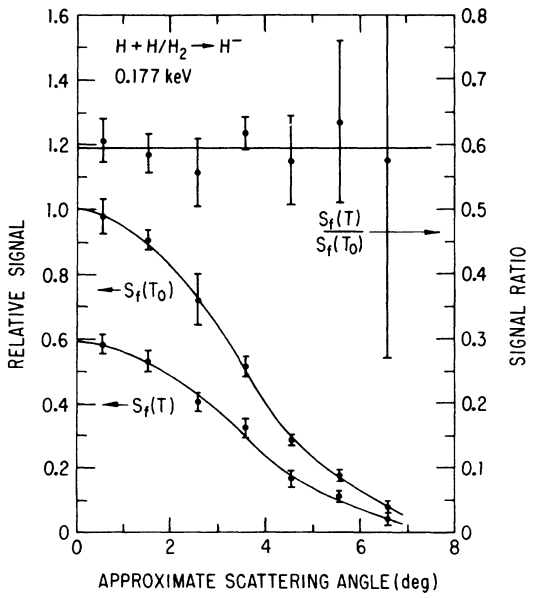

FIG. 3. Relative values of H^- signals $S_f(T_0)$ and $S_f(T)$ and their ratios vs approximate scattering angle.

IV. FINAL CROSS-SECTION DATA AND DISCUSSION

The results of the σ_{01} investigations made here for H impact on H and H_2 targets are presented in Table I. The σ_m data and their uncertainties were taken directly from the work of Van Zyl *et al.*[1] The σ_a/σ_m values were obtained from the measured $S_f/(T)/S_f(T_0)$ using Eq. (2), and their uncertainties were determined by quadrature combination of all the (uncorrelated) individual uncertainties known to be present in the measurement and data-analysis procedures employed. The tabulated σ_a values were obtained directly from the products of σ_m and σ_a/σ_m, whose uncertainties were combined in quadrature to obtain those for σ_a. These results are compared with other work in Fig. 4, and can be easily identified by their plotted uncertainties.

As can be seen, our σ_{01} data for H + H collisions are in generally good agreement with the data of McClure,[16] with the obvious exception of his lowest-H-energy data point. In fact, because the σ_m values of McClure[16] are slightly smaller than those of Van Zyl *et al.*[1] for H energies near 2 keV, the agreement between the two σ_a/σ_m is quite exceptional. Our agreement with the work of Hill *et al.*[17] is less pleasing (although within mutual uncertainties), but again, these two sets of σ_a/σ_m agree better than the σ_a values themselves.

Unfortunately, we know of no other experimental results (or detailed theoretical calculations) with which to compare our data at the lower H energies. Note, however, that the H-energy dependence of σ_{01} appears to be quite different for H and H_2 targets, with σ_a crossing over and exceeding σ_m for H energies below about 0.2 keV. We shall return later to a discussion of this feature.

Our results for σ_{0-1} are presented in Table II. Here, the σ_m value listed at 2-keV H energy is that reported by Hill *et al.*,[17] and the results for H energies below

TABLE I. Electron-loss cross sections for H impact on H and H_2.

E (keV)	σ_m (10^{-17} cm^2)	σ_a/σ_m	σ_a (10^{-17} cm^2)
2.000	7.48±15%	0.299±18%	2.24±23%
1.414	5.42±15%	0.292±35%	1.58±38%
1.000	3.72±15%	0.291±15%	1.08±21%
0.707	2.18±15%	0.353±34%	0.770±37%
0.500	1.16±15%	0.440±33%	0.510±36%
0.354	0.631±15%	0.532±29%	0.336±32%
0.250	0.330±15%	0.744±25%	0.246±29%
0.177	0.176±20%	1.05±47%	0.185±51%
0.125	0.086±25%	1.97±34%	0.169±42%

0.35-keV H energy were again taken from the data of Van Zyl *et al.*[1] The values at the intermediate H energies are those obtained here, using the procedure outlined in Sec. III. The values of σ_a/σ_m and σ_a and their uncertainties were obtained in the same way as described above for the σ_{01} data.

Our data for these ion-pair-formation reactions are compared with other results in Fig. 5. As can be seen, the new results obtained here for H_2 targets merge smoothly onto the data of McClure[20] and Hill *et al.*[17] for H energies above 2 keV, and onto the data of Van Zyl *et al.*[1] for H energies below 0.4 keV. For the case of H targets, our σ_{0-1} are again in agreement at the higher H energies with those of McClure[16] and of Hill *et al.*,[17] at least to within measurement uncertainties. Note that, as for H_2 targets, this ion-pair-formation process,

$$H+H \rightarrow H^+ + H^- , \tag{7}$$

is again characterized by a large cross-section structure for H energies below about 1 keV.

This large structure, however, was not predicted by the calculations of Borondo *et al.*,[25] shown here as the dotted-line curve in Fig. 5, even though their approach was based upon a molecular picture of this low-energy interaction. These workers attribute their overestimate of the cross section at the higher H energies to the fact that they actually calculated σ_{0-1} plus (approximately) $\frac{1}{4}$ of the electron-stripping cross section, σ_{ES}, for the reaction

$$H+H \rightarrow H^+ + e^- + H . \tag{8}$$

In fact, by using the σ_{01} data of McClure[16] to estimate σ_{ES}, they present an "adjusted" σ_{0-1} which is in reasonable agreement with the σ_{0-1} measured by McClure[16] for H energies above about 5 keV.[26]

However, such "adjustments" obviously cannot account for the severe discrepancy between these calculations and our σ_{0-1} data at the lower H energies. Indeed, these two sets of results differ by a factor of about 50 at 0.25-keV H energy. It thus appears that the large low-H-energy structure in this cross section must result from some interaction channel(s) not included in the theoretical model.

Borondo *et al.*[25] did not include coupling through any intermediate molecular states above those leading to $H(1s)+H(2s,2p)$ in the separated-atom (SA) limit. We would be surprised if the states leading to $H(1s)+H(nd,m_l=0)$, for example, were not involved here. These states are nearly energy degenerate with the $H^+ + H^-$ molecular state at large internuclear separation. Also, the $H(nd,m_l=0)$ wave functions have extended "lobes" which should be aligned with the internuclear axis during the interaction, in the same region where the H^- electrons in the Coulomb state are probably concentrated. We have found that for H impact on Ar and Kr targets, the cross sections for $H^*(nd)$ population seem to be related to the transient existence of similar Coulomb molecular states during the interactions,[27]

TABLE II. Electron-capture cross sections for H impact on H and H_2.

E (keV)	σ_m (10^{-18} cm^2)	σ_a/σ_m	σ_a (10^{-18} cm^2)
2.000	6.70±15%	0.357±23%	2.39±27%
1.414	3.69±18%	0.359±38%	1.33±42%
1.000	2.13±18%	0.344±42%	0.733±45%
0.707	1.45±21%	0.513±34%	0.744±40%
0.500	1.61±18%	0.357±34%	0.575±39%
0.354	2.04±18%	0.330±37%	0.673±41%
0.250	2.51±18%	0.390±26%	0.979±32%
0.177	3.06±18%	0.354±30%	1.08±35%
0.125	3.01±20%	0.420±28%	1.26±34%
0.088	2.10±22%	0.668±35%	1.40±41%
0.063	1.65±24%	0.686±46%	1.13±52%

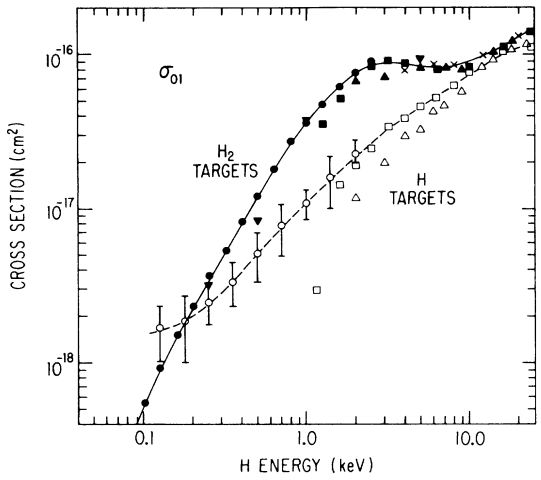

FIG. 4. Electron-loss cross sections for H impact on H and H_2. The measured data are from ○, present results; ●, Van Zyl *et al.* (Ref. 1); ▼, Smith *et al.* (Ref. 14); ×, Stier and Barnett (Ref. 15); ■, □, McClure (Ref. 16); and ▲, △, Hill *et al.* (Ref. 17).

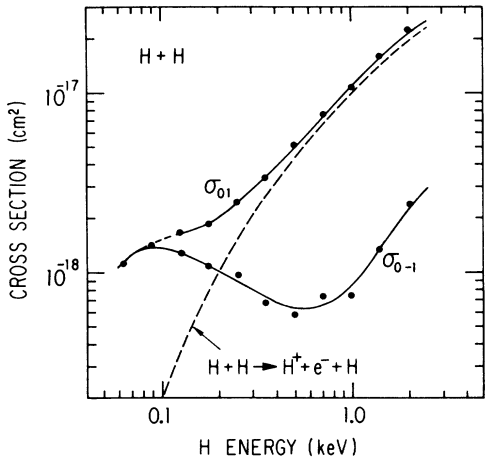

FIG. 6. Comparison of the electron-loss and electron-capture cross sections for H + H collisions. The dashed-line curve is the electron-stripping cross section deduced from $\sigma_{01}-\sigma_{0-1}$.

suggesting that such couplings may be quite strong at low H-impact energies.

The σ_{01} shown in Fig. 4 for H + H collisions is, of course, the sum of the cross sections for the reactions in Eqs. (7) and (8), while the σ_{0-1} shown in Fig. 5 is for the reaction in Eq. (7) only. It is thus of interest to compare these data directly to see what can be learned about the electron-stripping cross section σ_{ES}. Such a comparison is presented in Fig. 6.

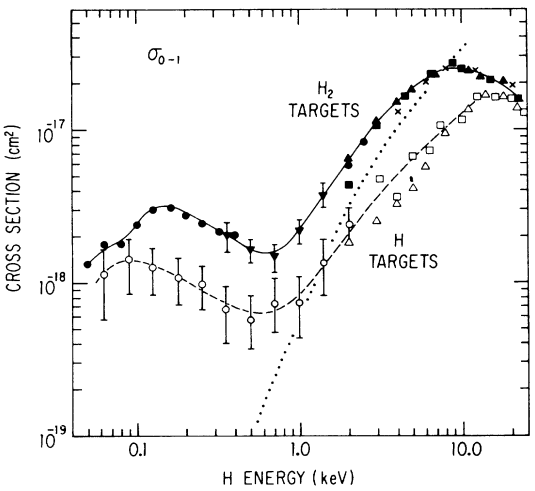

FIG. 5. Electron-capture cross sections for H impact on H and H_2. The measured data are from ▼, ○, present results; ●, Van Zyl *et al.* (Ref. 1); ×, Stief and Barnett (Ref. 15); ■, □, McClure (Ref. 20); and ▲, △, Hill *et al.* (Ref. 17). The dotted-line curve is the theory of Borondo *et al.* (Ref. 25).

As can be seen, even though we could not here obtain σ_{01} data for H energies below 0.125 keV,[28] there is little doubt that σ_{01} and σ_{0-1} are approaching one another at the lower H energies. Their difference, σ_{ES}, shown by the dashed-line curve, is a smoothly decreasing function of H energy (similar, in fact, to the σ_{01} data for H_2 targets shown in Fig. 4). Clearly the ion-pair-formation reaction is the dominant mechanism resulting in charged collision products at low interaction energies, as has been found earlier for low-energy H collisions with other targets.[1,3] We sincerely hope that these results will now lead to additional theoretical work to elucidate this interesting situation.

Finally, we believe that this very agreement speaks well for our correct assessment of the numerous experimental difficulties encountered during these measurements. If the influence of product-ion angular scattering, for example, or the background-charged-particle signals (which were generally somewhat different for the σ_{01} and σ_{0-1} measurements) had been improperly accounted for, it would be somewhat fortuitous to have obtained such self-consistent data as those shown in Fig. 6.

ACKNOWLEDGMENTS

The authors express their thanks to H. Neumann and R. C. Amme for their contributions to these measurements. This work has been supported by the Aeronomy Program, Division of Atmospheric Sciences, National Science Foundation, the Boettcher Foundation, and the Donald H. Menzel Endowment Fund at the University of Denver.

*Present address: Department of Physics and Astronomy, University of Nebraska, Lincoln, NE 68588.

[1]B. Van Zyl, T. Q. Le, and R. C. Amme, J. Chem. Phys. **74**, 314 (1981).

[2]M. W. Gealy and B. Van Zyl, preceding paper, Phys. Rev. A **36**, 3091 (1987).

[3]B. Van Zyl, T. Q. Le, H. Neumann, and R. C. Amme, Phys. Rev. A **15**, 1871 (1977).

[4]B. Van Zyl, N. G. Utterback, and R. C. Amme, Rev. Sci. Instrum. **47**, 814 (1976).

[5]B. Van Zyl and M. W. Gealy, Rev. Sci. Instrum. **57**, 359 (1986).

[6]We used a Keithley model 642 electrometer, generally operated in the "rate-of-charge" mode. We had no way to accurately test the absolute sensitivity of this device, although we seriously doubt that its readings were in error by more than ± 10 to $\pm 15\%$. This was not in general a problem, however, for the electrometer was used primarily to measure relative signal magnitudes.

[7]Fortunately, most of these ions were quite energetic, being produced by electron-impact ionization of H_2 in the region near the furnace tube, which was operated up to $+1000$ volts above ground (Ref. 5). Thus, they moved rapidly through the interaction region into the quadrupole chamber (see Fig. 1 of paper I), where a strategically oriented baffle at variable potential was used to minimize the probability of their reemerging from this chamber.

[8]Much of this background signal resulted from these charged particles being accelerated towards, and impacting on, the surfaces of these charge-state separators. Here, they released additional secondary electrons and ions, which had a rather direct path for entering the ion collectors at energies equivalent to the potential applied to the separator plate where they originated.

[9]In addition to preventing escape of secondary electrons from the Faraday cups, these potentials served to keep negatively charged particles from entering the collectors. Unfortunately, however, they also tended to draw in positive ions.

[10]M. W. Gealy, Ph.D. thesis, University of Denver, 1986.

[11]As we did in Sec. III of paper I, we assume for this discussion that the ion signals resulting from H impact on the background-gas particles present in the scattering chamber have been suitably subtracted, as they were during the actual data analysis.

[12]This "signal" came primarily from the effects of environmental temperature changes (piezoelectric effects) on the feedthrough header used to pass the small signal currents through the vacuum wall. In spite of all the water cooling employed around the furnace tube and its vacuum-chamber housing (see Fig. 1 of paper I), we were never able to eliminate completely this apparent signal.

[13]Even under the best of conditions, we typically were forced to reject about 20% of the data runs made, because the differences between these two $S_f(T_0)$ values were statistically unacceptable. This usually happened on the first data run of the day, when the thermal drifts in the system were the most severe (see Ref. 12), but sometimes on other occasions as well. Because this measurement procedure involved so much duplication, and the data were carefully reduced by hand as they were being acquired, we were usually able to identify any spurious signals rather quickly.

[14]K. A. Smith, M. D. Duncan, M. W. Geis, and R. D. Rundel, J. Geophys. Res. **81**, 2231 (1976).

[15]P. M. Stier and C. F. Barnett, Phys. Rev. **103**, 896 (1956).

[16]G. W. McClure, Phys. Rev. **166**, 22 (1968).

[17]J. Hill, J. Geddes, and H. B. Gilbody, J. Phys. B **12**, 3341 (1979).

[18]It was not possible here to plot all the available data for this reaction at higher H energies, or even more than a few representative data points from each of the references cited.

[19]At 2-keV H energy, we actually measured an apparent $\sigma_{01}=7.92\times10^{-17}$ cm^2, about 5.9% above the value 7.48×10^{-17} cm^2 reported by Van Zyl *et al.* (Ref. 1). However, this measurement depended directly on the accuracy of the electrometer used (which, as noted in Ref. 6, was not calibrated here). We thus concluded that it was most appropriate to use the σ_{01} measurement of Van Zyl *et al.* (Ref. 1) as a standard for this comparison.

[20]G. W. McClure, Phys. Rev. **134**, A1226 (1964).

[21]To be consistent, the apparent σ_{0-1} values plotted here have been reduced to 5.9% below the actual measured values, for the same reason discussed above in Ref. 19.

[22]J. F. Williams, Phys. Rev. **153**, 116 (1967).

[23]Van Zyl *et al.* (Ref. 1, see Fig. 8) have compared the cross sections for production of various charged particles in $H+H_2$ collisions. We believe these data to be correct as presented, except that the minimum in σ_{0-1} for H energies between about 0.4 and 2.5 keV is not as "deep" as shown.

[24]We were unable to acquire statistically meaningful data of this type at still lower H energies, the signals at larger scattering angles simply being too small to allow a definitive determination of their ratio. However, because Figs. 1 and 2 indicate that the loss of ion signal from angular-scattering effects at the lower H energies E scaled approximately as E^{-1}, we scaled the H-energy dependence of such uncertainties in the same way.

[25]F. Borondo, F. Martín, and M. Yáñez, Phys. Rev. A **35**, 60 (1987).

[26]However, if a similar procedure is followed using the σ_{01} data shown in Fig. 4, the resulting σ_{0-1} becomes negative for H energies below a few keV.

[27]B. Van Zyl and M. W. Gealy, Phys. Rev. A **35**, 3741 (1987), and included references to our earlier work.

[28]This resulted from the very rapid decrease of σ_{01} for $H+H_2$ collisions with H energy. In other words, the σ_m was too small to allow a definitive σ_a/σ_m measurement.